Elaboration and characterization of a KCl single crystal doped with nanocrystals of a Sb_2O_3 semiconductor*

L. Bouhdjer[1, †], S. Addala[1], A. Chala[2], O. Halimi[1], B. Boudine[1], and M. Sebais[1]

[1]Laboratory of Crystallography, Department of Physics, Mentouri- University of Constantine, Constantine 25000, Algeria
[2]Laboratory Applied Chemistry, Department of Chemical, Mohamed Khaider- University of Biskra, Biskra 07000, Algeria

Abstract: Undoped and doped KCl single crystals have been successfully elaborated via the Czochralski (Cz) method. The effects of dopant Sb_2O_3 nanocrystals on structural and optical properties were investigated by a number of techniques, including X-ray diffraction (XRD), scanning electron microscopy (SEM), energy dispersive X-ray (EDAX) analysis, UV-visible and photoluminescence (PL) spectrophotometers. An XRD pattern of KCl:Sb_2O_3 reveals that the Sb_2O_3 nanocrystals are in the well-crystalline orthorhombic phase. The broadening of diffraction peaks indicated the presence of a Sb_2O_3 semiconductor in the nanometer size regime. The shift of absorption and PL peaks is observed near 334 nm and 360 nm respectively due to the quantum confinement effect in Sb_2O_3 nanocrystals. Particle sizes calculated from XRD studies agree fairly well with those estimated from optical studies. An SEM image of the surface KCl:Sb_2O_3 single crystal shows large quasi-spherical of Sb_2O_3 crystallites scattered on the surface. The elemental analysis from EDAX demonstrates that the KCl:Sb_2O_3 single crystal is slightly rich in oxygen and a source of excessive quantities of oxygen is discussed.

Key words: Sb_2O_3 semiconductor; KCl single crystal; Cz method; XRD; SEM; UV-vis absorption
DOI: 10.1088/1674-4926/34/4/043001 **EEACC:** 2520

1. Introduction

Research on nano-semiconductors has increased remarkably in the past few years due to their unique chemical, physical and biological characteristics, and thus behaves differently, with respect to materials of a coarser structure, even when the element or molecular composition is the same. The remarkable behavior of a nano-semiconductor demonstrates due to the quantum confinement effect of charges. The term, quantum confinement effect, was introduced to explain a wide range of properties of the nanostructure of semiconductors in response to changes in dimension or shapes within nanoscales[1−6]. The group V–VI binary compounds are highly anisotropic semiconducting materials[7]. Among these binaries a few different antimony oxides exist such as Sb_2O_3, Sb_2O_4, Sb_2O_5 and Sb_6O_{13}[8]. As an important antimony oxide (Sb_2O_3) has experienced a heightened interest due to its indirect band gap energy of 3.3 eV and has a number of applications in various industries. It can be used as a very good catalyst[9], efficient fire retardant[10], fining agent[11], filler and optical material[12, 13]. Due to higher proton conductivity, hydrous Sb_2O_3 may have a possible application as the humidity sensor[14]. Moreover, the Sb_2O_3 thin film behaves as an n-type semiconductor which invites photovoltaic applications[15], and important nonlinear optical properties of glasses doped by Sb_2O_3[16−18].

The study of the optical properties of a nano-semiconductor in ionic solids can be very conveniently carried out on the simplest compounds, alkali halides AX were A: alkali cation and X: halogen anion. They offer a number of advantages such as a simple structure, high degree of chemical purity, easy manipulation and wide range of doping impurities with different concentrations. On the other hand, their high gap energy ($\sim$ 10 eV) provides a large window for optical spectroscopy. However, there is a little research on nano-semiconductors doped in crystalline hosts. In the case of alkali halides, earlier studies have been reported on KBr:ZnO, NaCl:CdS and KBr:CdTe single crystals[19−21]. Samah *et al.*[22] have analyzed alkali halides (KBr, NaCl) doped with II–VI and I–VIII semiconductors like ZnO, AgBr and CuCl.

In the present paper, KCl and KCl:Sb_2O_3 single crystals have been successfully elaborated by the CZ method. The structural and optical properties of these crystals were investigated. The doping effects of the Sb_2O_3 nano-semiconductor on structural and optical properties of KCl single crystals were observed and highlighted.

2. Experimental details

KCl and KCl:Sb_2O_3 single crystals were prepared using the CZ method. In the present work, KCl powder was procured from the "LABOSI/Chemicals products and reaction laboratory" with 99.9% purity, and Sb_2O_3 nano-powder was procured from "Aldrich chemicals" with 99.99% purity. The KCl:Sb_2O_3 single crystal was prepared with 1 mol% of Sb_2O_3 nano-powder and 99% mol of KCl, these mixtures were heated in a crucible to melt. The oven temperature has been controlled by the control system: controller [REX-C100 SEPIES] and the platinum/platinum radium (10%) thermocouple, the pulling rate was in the 8–10 mm/h range and the rotation speed was V_r = 1 round/min. During the growth, changing the thermal gradient to control the diameter of the KCl and KCl:Sb_2O_3 (1, 5 cm) with length 5 cm.

* Project supported by the Crystallography Laboratory of the University of Constantine, Algeria.
† Corresponding author. Email: bouhdjerlazhar@gmail.com
Received 20 September 2012, revised manuscript received 17 October 2012

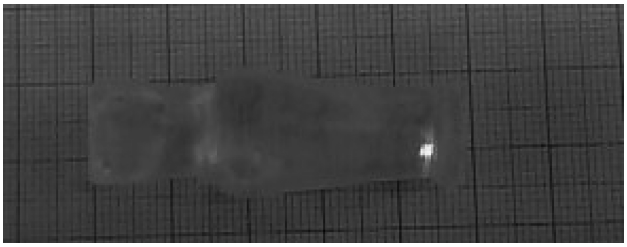

Fig. 1. Photograph of a KCl:Sb_2O_3 single crystal.

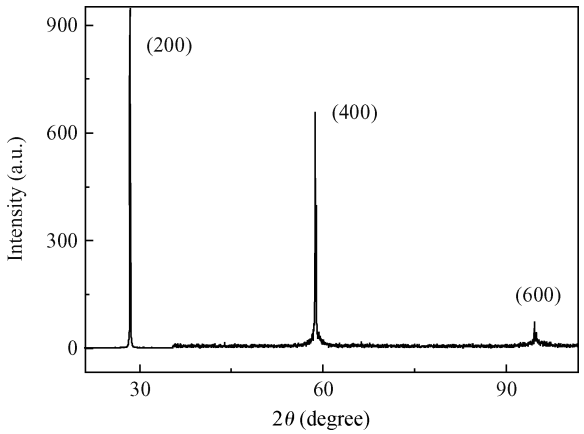

Fig. 2. XRD pattern of a pure KCl single crystal.

The growth is carried out following the crystallography [100] axes. The obtained crystals are cleaved parallel to the (100) plane with the required size. Figure 1 displays a photograph of a KCl:Sb_2O_3 single crystal. The thermal treatment of KCl:Sb_2O_3 samples is performed at 550 ℃ for 24 h under atmospheric air. After the annealing, the samples are cooled slowly at room temperature.

XRD data have been obtained using CuKα radiation ($\lambda_{K\alpha}$ = 1.5402 Å) and a graphite filter with the BRUKER-AXS D8 diffractometer. The surface morphology of the samples was analyzed using a scanning electron microscope (SEM) at 15 kV accelerating voltages. Quantitative analyses were obtained by an energy dispersive X-ray analysis (EDAX) with acceleration voltage 15 kV. The optical properties were analyzed using an UV–visible spectrophotometer (Shimadzu, UV-3101). Furthermore, the photoluminescence (PL) was measured at room temperature (RT) and the samples were excited by a laser (ionized light E_{ex} = 270 nm) with an output power of 10 mW.

3. Results and discussion

XRD studies have been performed on samples of pure KCl and KCl:Sb_2O_3 crystals to determine their crystallographic structure. Figure 2 shows the XRD diagram of a pure KCl single crystal. It exhibits three intense peaks at 2θ = 28.48°; 2θ = 58.78° and 2θ = 95° corresponding to the plan (200) and its harmonics (400) and (600) respectively. This result shows that the KCl crystal has a cubic structure with the symmetry of a Fm3m space group. By referring to data from the JCPDS 41-1476 file, it discloses that the sample has a single crystal character and confirms that the crystal was cleaved parallel to the (100) plane.

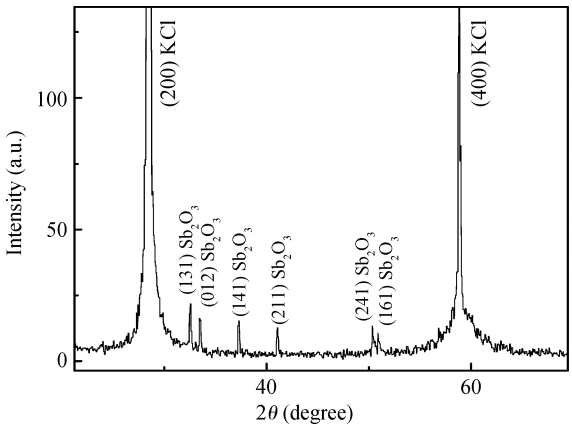

Fig. 3. XRD pattern of a KCl:Sb_2O_3 single crystal.

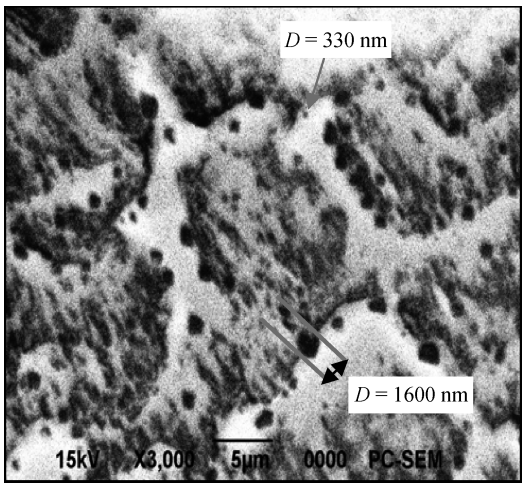

Fig. 4. SEM image of a KCl:Sb_2O_3 single crystal after annealing at 550 ℃ (24 h) in air atmosphere.

Table 1. Crystallites sizes calculated from the XRD.

2θ(°)	32.56	33.51	37.29	41.07	50.37	50.09
(hkl)	(131)	(012)	(141)	(211)	(241)	(161)
D (nm)	60.17	58.95	60.8	93.26	80.52	74.12

Figure 3 displays the XRD spectrum of the KCl:Sb_2O_3 samples. Aside from the peaks related to the KCl host, it contains six broad peaks indexed the Sb_2O_3 orthorhombic phase with the symmetry of Pccn and cell parameters a = 4.91 Å, b = 12.45 Å and c = 5.41 Å (JCPDS Card No. 11-0691). The appreciate intensity of these peaks indicates a high crystalline quality of Sb_2O_3. This result demonstrates the incorporation of Sb_2O_3 into the KCl host. Moreover, the absence of peaks corresponding to another phase such as $Sb_4O_5Cl_2$ or $SbCl_3$ indicates that there was no chemical reaction between Sb_2O_3 and KCl in spite of the high temperature of growth.

Table 1 presents the average sizes of crystallites corresponding to each diffracting plan. The average radius found is about 71.30 nm.

The surface morphology of KCl:Sb_2O_3 is studied by SEM and is shown in Fig. 4. The morphology displays a quasi-spherical shape of Sb_2O_3 crystallites scattered on the surface of KCl. The mean crystallite size obtained using Scheerer's for-

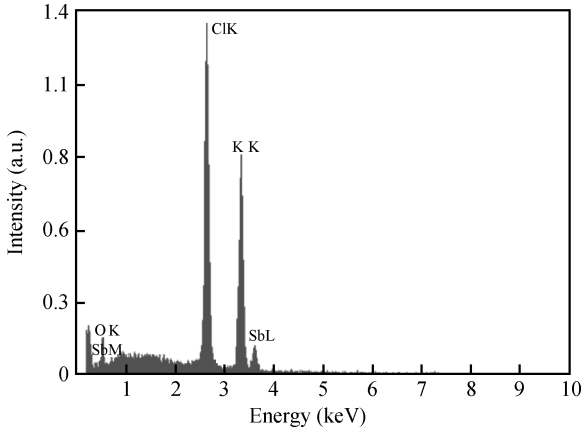

Fig. 5. Typical EDAX pattern of a KCl:Sb_2O_3 single crystal after annealing at 550 ℃ (24 h) in atmospheric air.

Table 2. Overage atomic percentage of a KCl:Sb_2O_3 single crystal after annealing.

Element	wt%	at%
OK	0.86	2.03
ClK	45.18	48.26
KK	49.98	48.47
SbL	3.98	1.24
Matrix	Correction	ZAF

mula is in all cases substantially smaller than the dimension of grains observed by the SEM image, indicating that these grains are probably an aggregation of many crystallites of Sb_2O_3.

The energy dispersive X-ray analyses (EDAX) spectrum (Fig. 5) indicating the presence of K, Cl, Sb and O elements and no other elements were detected, which demonstrates that the KCl:Sb_2O_3 single crystal has a very high purity. However, the average atomic percentage (Table 2) shows that the crystal is slightly rich in oxygen. The source of the excessive quantities of oxygen are attributed to the high solubility of O_2 molecular in the KCl:Sb_2O_3 crystals after annealing at 550 ℃ (24 h) in atmospheric air.

Figure 6(a) shows the optical absorption spectra of a pure KCl single crystal (without annealing). It is transparent in the visible region and has a strong absorption in the near ultraviolet, and we have not detected any broad absorption relative to a color center. The absorption edge ($E_g \approx 6.20$ eV) is determined by the second derivative method[23] presented in Fig. 6(b).

Figure 7 shows the optical absorption spectrum of a KCl:Sb_2O_3 crystal after annealing at 550 ℃ (24 h) in atmospheric air where two absorption bands appear centered at 334 nm (3.71 eV) and 453 nm (2.74 eV) the first absorption band can be assigned to intra-3d transition of Sb^{+3} in the orthorhombic structure of Sb_2O_3[24] and the second band indexed O_2^- color center respectively[25]. The Sb_2O_3 nanocrystals have an orthorhombic structure and the orthorhombic Sb_2O_3 bulk crystal has a band gap energy of 3.3 eV[26]. It is well known that the energy gap of the semiconductor nanocrystals increases with the decrease in grain size, which can be attributed to the quantum confinement effects. In our study, the size of the Sb_2O_3 nanocrystals is not small enough, but the quasi-spherical Sb_2O_3 nanostructures still develop quantum con-

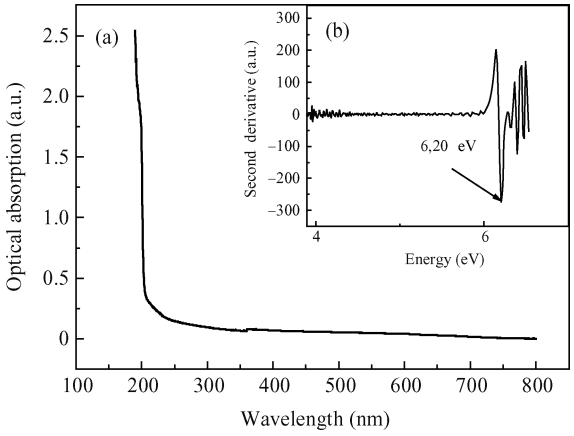

Fig. 6. (a) Optical absorption spectrum of pure KCl crystal (without annealing), and (b) E_g of KCl crystal determined by the second derivative.

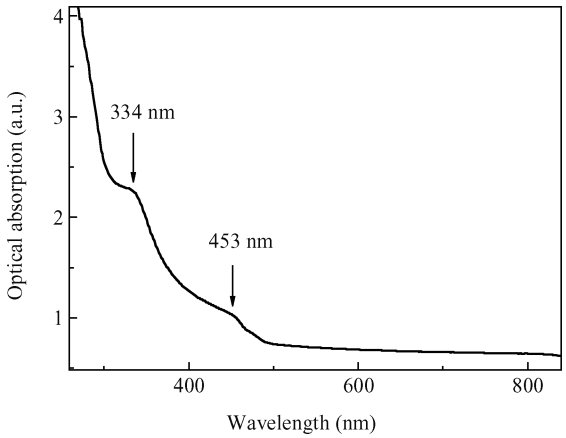

Fig. 7. Optical absorption spectra of a KCl:Sb_2O_3 single crystal after annealing at 550 ℃ (24 h) in atmospheric air.

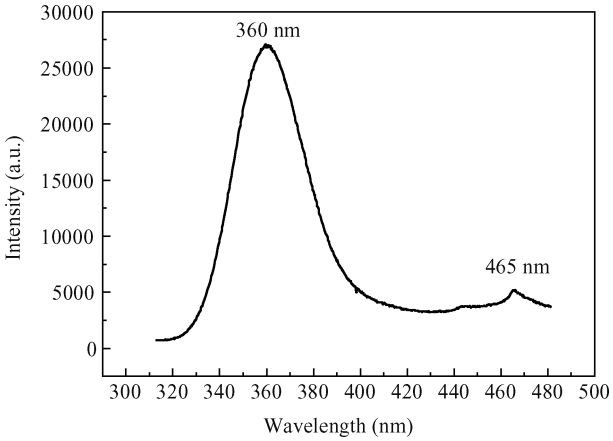

Fig. 8. Room temperature PL of a KCl:Sb_2O_3 single crystal after annealing at 550 ℃ (24 h) in atmospheric air.

finement effects on the blue-shift of absorption edge $\Delta E_g = 0.41$ eV. Furthermore, the existence of a O_2 color center confirmed the incorporation of the KCl:Sb_2O_3 crystal by O_2 during annealing under atmospheric air which is consistent with EDAX analyses of KCl:Sb_2O_3.

Figure 8 displays the photoluminescence (PL) spectrum of the KCl:Sb_2O_3 crystal at (RT) after annealing at 550 ℃ (24 h) under atmospheric air, it shows a broad emission band centered at 360 nm (3.44 eV) relative to Sb_2O_3 nanocrystals with a blue-shift $\Delta E_g = 0.14$ eV and another peak located at 456 nm (2.72 eV) indexed the O_2^- color center, in concordance with the optical absorption measurement. Moreover, the strong PL intensity from the Sb_2O_3 nanocrystals included in KCl can be attributed to their high crystallization and to their good surface, which is in agreement with the XRD patterns of KCl:Sb_2O_3 discussed earlier. In addition; the enlargement of the band relative to Sb_2O_3 can be explained by the presence of size dispersion of Sb_2O_3 nanocrystals inside KCl (Table 1).

4. Conclusion

Both pure KCl single crystals and crystals doped with Sb_2O_3 nanocrystals were prepared by the Cz method. Structural characterization by XRD shows the incorporation of the KCl host by Sb_2O_3 nanocrystals. Furthermore, SEM images present large quasi-spherical particles of Sb_2O_3 and the (EDAX) analyses indicate the high purity of a KCl:Sb_2O_3 single crystal submitted to annealing in atmospheric air, except for slightly excessive quantities of oxygen it has good stoichiometrics. In addition, the optical absorption spectra of KCl:Sb_2O_3 submitted to annealing shows a band located at 334 nm revealing Sb_2O_3 nanocrystals with a blue shift from the bulk gap of $\Delta E_g = 0.41$ eV and other broadly located at 435 nm due to the O_2^- color center. In addition, the photoluminescence spectra at RT shows two luminescence bands, the first located at 360 nm, with displacement e.g. towards the short wavelength due to the nanometric size of Sb_2O_3, and the second band located at 465 nm revealing an O_2^- color center which is consistent with optical absorption and EDAX analyses.

Acknowledgements

The authors thank Prof. A. B. Chala for his assistance.

References

[1] Brus L E. Electronic wave functions in semiconductor clusters: experiment and theory. Chem Phys, 1986, 90: 2555
[2] Lieber C M. One-dimensional nanostructures: chemistry, physics and application. Solid State Commun, 1998, 107: 607
[3] Smalley R E, Yakobson B I. The future of the fullerenes. Solid State Commun, 1998, 107: 597
[4] Schneider J J. Nanomaterials: synthesis, properties and applications. Adv Mater, 2004, 9: 997
[5] O'Regan B, Gratzel M. A low-cost, high-efficiency solar cell based on dye-sensitized colloidal TiO_2 films. Letters to Nature, 1991, 353: 737
[6] Colvin V L, Schlamp M C, Aliviastos A P. Light-emitting diodes made from cadmium selenide nanocrystals and a semiconducting polymer. Letters to Nature, 1994, 370: 354
[7] Wyckoff R W G. Crystal structure. 2nd ed. New York: Wiley, 1994
[8] Orosel D, Balog P, Liu H, et al. Sb_2O_4 at high pressures and high temperatures. Solid State Chem, 2005, 178: 2602
[9] Nanda K K, Sahu S N, Behera S N. Liquid-drop model for size-dependent melting of low-dimensional systems. Phys Rev, 2002, A66: 013208
[10] Mahdavian A R, Morshedian J, Rezaie M. The comparison between synergistic effect of Sb_2O_3 and $Al(OH)_3$ on the flame-retardancy of HIPS in the presence of tetrabromobisphenol-A. Iranian Polymer, 2004, 13: 219
[11] Grund, Jonson B. Compositional effect on fining and oxygen activity in mixed alkali silicate glass. Journal of Glass Science and Technology Part A, 2009, 50(1): 62
[12] Haberland H, Insepov Z, Moseler M. Molecular-dynamics simulation of thin-film growth by energetic cluster impact. Phys Rev, 1995, B51: 11061
[13] Fuchs G, Melinon P, Santos Aires F, et al. Cluster-beam deposition of thin metallic antimony films: cluster-size and deposition-rate effects. Phys Rev, 1991, B44: 3926
[14] Burguer P A, Cuendet P, Gratzel M. Ultrafine and specific catalysts affording efficient hydrogen evolution from water under visible light illumination. Am J Chem Soc, 1981, 103: 2923
[15] Meticos-Hucovic M, Loveric B. Semiconducting properties of anodically formed layer on antimony. Electrochim Acta, 1978, 23: 1371
[16] Nalin M, Poulain M, Riberio J L, et al. Antimony oxide based glasses. Non-Cryst Solids, 2001, 284: 110
[17] Kim H J, Lee S H, Yon S J, et al. Effect of Sb_2O_3 on solarization of photosensitive glasses containing Ag and CeO. Korean J Ceram, 2001, 7: 58
[18] Satyanarayana T, Kityk I V, Ozga K, et al. Role of titanium valence states in optical and electronic features of PbO–Sb_2O_3–B=O_3:TiO_2 glass alloys. Alloys Compd, 2009, 482: 283
[19] Halimi O, Boudine B, Sebais M, et al. Structural and optical characterization of ZnO nanocrystals embedded in bulk KBr single crystal. Mater Sci Eng C, 2003, 23: 111
[20] Boudine B, Sebais M, Halimi O, et al. Structural and optical properties of CdS nanocrystals embedded in NaCl single crystals. Mouras R Catalysis Today, 2004, 89: 293
[21] Bensouici A, Plaza J L, Diéguez E, et al. CdTe aggregates in KBr crystalline matrix. Luminescence, 2009, 129: 948
[22] Samah M, Khalfane H, Bouhuerra, et al. Optic and structural properties of the aggregations of AgBr in an ionic matrix. Annales de Chimie Science des Matériaux, 2004, 29: 49
[23] Othmani A, Plenet J C, Berstein E, et al. Nanocrystals of CdS dispersed in a sol–gel silica glass: optical properties. J Cryst Growth, 1994, 144: 141
[24] Ge S, Wang Q, Li J, et al. Controllable synthesis and formation mechanism of bow-tie-like Sb_2O_3 nanostructures via a surfactant-free solvothermal route. Alloys and Compounds, 2010, 494: 169
[25] Zehani F, Sebais M. UV-visible emission of $(O_2 - F^+)$ centers in KBr. Cryst Res Technol, 2007, 42: 1123
[26] Naidu B S, Pandey M, Sudarsan V, et al. Interaction of Sb^{+3} ions with Eu^{+3} ions during the room temperature synthesis of luminescent Sb_2O_3 nanorods: probed through Eu^{+3} luminescence. Luminescence, 2010, 113: 177